

## Small molecule mimetics of an interferon- $\alpha$ receptor interacting domain



Angelica M. Bello<sup>a,b,d</sup>, Lianhu Wei<sup>a,b,d</sup>, Beata Majchrzak-Kita<sup>b</sup>, Noruê Salum<sup>a,f</sup>, Meena K. Purohit<sup>a,g</sup>, Eleanor N. Fish<sup>b,c,†</sup>, Lakshmi P. Kotra<sup>a,b,d,e,\*,†</sup>

<sup>a</sup> Center for Molecular Design and Preformulations, University Health Network, Toronto, Ontario M5G 1L7, Canada

<sup>b</sup> Toronto General Research Institute, Toronto, Ontario M5G 2M1, Canada

<sup>c</sup> Department of Immunology, University of Toronto, Toronto, Canada

<sup>d</sup> Department of Pharmaceutical Sciences, Leslie Dan Faculty of Pharmacy, University of Toronto, Toronto, Ontario, Canada

<sup>e</sup> McLaughlin Center for Molecular Medicine, University of Toronto, Toronto, Ontario, Canada

<sup>f</sup> Federal University of Paraná, Curitiba, Paraná, Brazil

<sup>g</sup> Department of Pharmacy, Birla Institute of Technology & Science, Pilani 333 031, India

### ARTICLE INFO

#### Article history:

Received 17 October 2013

Revised 12 December 2013

Accepted 21 December 2013

Available online 2 January 2014

#### Keywords:

Interferon

Peptidomimetics

IFN- $\alpha$  receptor

### ABSTRACT

Small molecules that mimic IFN- $\alpha$  epitopes that interact with the cell surface receptor, IFNAR, would be useful therapeutics. One such 8-amino acid region in IFN- $\alpha$ 2, designated IRRP-1, was used to derive 11 chemical compounds that belong to 5 distinct chemotypes, containing the molecular features represented by the key residues Leu30, Arg33, and Asp35 in IRRP-1. Three of these compounds exhibited potential mimicry to IRRP-1 and, in cell based assays, as predicted, effectively inhibited IFNAR activation by IFN- $\alpha$ . Of these, compound **3** did not display cell toxicity and reduced IFN- $\alpha$ -inducible STAT1 phosphorylation and STAT-DNA binding. Based on physicochemical properties' analyses, our data suggest that moieties with acidic pKa on the small molecule may be a necessary element for mimicking the carboxyl group of Asp35 in IRRP-1. Our data confirm the relevance of this strategy of molecular mimicry of ligand-receptor interaction domains of protein partners for small molecule drug discovery.

© 2014 Elsevier Ltd. All rights reserved.

## 1. Introduction

Many fundamental cellular processes are regulated by protein-protein interactions (PPI) for normal physiological maintenance.<sup>1–3</sup> PPI are important effectors in different disease processes, since they either directly or indirectly influence pathogenesis.<sup>4–7</sup> These interactions which occur between two or more partner protein molecules are therefore candidate targets for drug design.<sup>8,9</sup> Small molecule drugs that modulate PPI present as promising intervention therapeutics. In this context, three types of small molecules may be envisioned depending on the type of influence they elicit with the partner proteins involved in the PPIs: (i) agonists, or small molecules that would exert a positive response after binding to one of the protein partners, to enable downstream signaling, (ii) antagonists that would block the response or the downstream signaling after binding to one of the protein partners, or (iii) molecules that would stabilize the PPI.<sup>10–12</sup> Cytokines present themselves as

proteins that could be targeted effectively by small molecule drugs in this way.

Cytokines are biological response modifier proteins that invoke responses in target cells, mediated by activation of their cognate cell surface receptors. Receptor activation, and therefore the downstream response, are determined by the specific three-dimensional structure of the ligand interaction domains for each cytokine. Interferons (IFNs) are a family of cytokines that exhibit antiviral, growth inhibitory and immunomodulatory activities.<sup>13–15</sup> Over the past several years, investigations to delineate the essential hot-spots on the surfaces of IFNs- $\alpha\beta$ , associated with receptor binding and activation of subsequent functional activities, have been undertaken.<sup>16–19</sup> IFN- $\alpha$  subtypes were systematically investigated to decipher the specific regions on their surface responsible for binding to the cognate receptor, IFNAR.<sup>20,21</sup> Specifically, IFN- $\alpha$ 2a has three non-contiguous peptide regions on its primary structure that are essential for binding to the two membrane spanning sub-units of IFNAR.<sup>16,18</sup> These groups of peptides, identified as IFN receptor recognition peptides (IRRP), are critical for the activity of IFNs (Fig. 1).<sup>17,22</sup>

Currently, as a biological therapeutic, IFN is administered by subcutaneous injection, due to the complexities associated with administering protein molecules as therapeutics. Consequently,

\* Corresponding author. Address: 5-356, Toronto Medical Discoveries Tower/ MaRS Center, 101 College Street, Toronto, Ontario M5G 1L7, Canada. Tel.: +1 (416) 581 7601; fax: +1 (416) 581 7621.

E-mail address: [lkotra@uhnres.utoronto.ca](mailto:lkotra@uhnres.utoronto.ca) (L.P. Kotra).

† Co-senior authors.

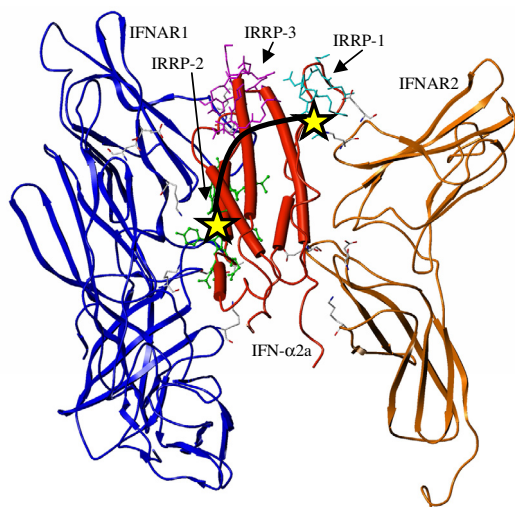


**Figure 1.** A model of the complex of IFN- $\alpha$ 2a (in red) with its receptor, IFNAR. IFNAR is a heterodimer represented by the two domains IFNAR1 (in blue) and IFNAR2 (in orange). Residues in IRRP-1, IRRP-2 and IRRP-3 regions are shown in capped stick models cyan, green and magenta, respectively, on IFN- $\alpha$ 2a. Potential strategy to design a complete mimic of IFN was to design individual IRRP regional mimics and tether them to mimic the interaction surfaces with IFNAR, illustrated by the stars in yellow with a tether.

the pharmaceutical and clinical challenges of these biologics lead to high treatment costs.<sup>23,24</sup> Thus, small non-protein molecule substitutes as mimics of IFNs would be an advantageous alternative, both for reducing the costs associated with a biological drug, and for increasing the ease of administration potentially via oral route.

As a first step towards designing a non-peptide mimetic of IFN- $\alpha$ 2a using in silico approaches, we undertook a systematic screen to identify small molecule structural mimics of each of the three IRRP regions on the surface of the IFN- $\alpha$ 2a protein.<sup>25</sup> Herein, we report the discovery of small molecules that mimic IRRP-1 and potentially bind to IFNAR2. We reveal a systematic process for screening a large set of molecules, and identify 11 compounds as potential mimics of IRRP-1. From this set of 11 compounds, and based on bioassays and cellular toxicity studies, we reveal unique small molecules that mimic surface residues on IFN- $\alpha$ 2a, that disrupt IFN-IFNAR binding. These findings serve as a foundation towards the larger goal of designing non-peptidic molecules as agonists for IFNAR.

## 2. Experimental section

### 2.1. Computer modeling

IRRP-1 in IFN- $\alpha$ 2a is comprised of residues Ser28-Cys29-Leu30-Lys31-Asp32-Arg33-His34-Asp35. Three structural features were selected from these residues to conduct small molecule chemical database searches, in order to identify small chemical compounds matching the surface features of IRRP-1 (Fig. 2). These molecular features are a hydrophobic character from the side chain of Leu30, a cationic center defined by the side chain of Arg33, and an anionic center defined by the carboxyl group of Asp35. The distance and volume tolerances for each feature were set in the range of 0.5–1 Å. Chemical databases used in the in silico screening include those from the commercial vendors and public sources, customized to work in our computational environment, and the combined library contained a total of 4.1 million compounds. In silico chemical database searches were performed using UNITY module embedded in SYBYL molecular modeling package (Tripos Inc./Certara Group).<sup>26</sup> A UNITY Flex search was conducted allowing

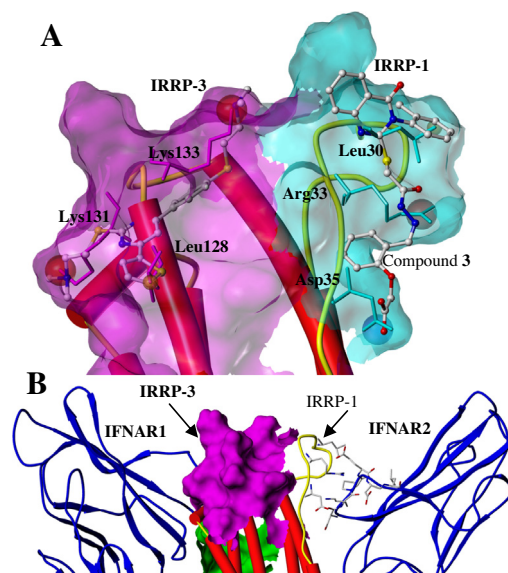


**Figure 2.** (A) Three dimensional structure of IFN- $\alpha$ 2a illustrating the key regions, IRRP-1 and IRRP-3 (cyan and magenta regions, respectively). These regions are illustrated by semi-transparent Connolly surfaces derived from the amino acid residues in IRRP-1 and IRRP-3 segments. Ball-and-stick model of compound **3**, derived from IRRP-1 residues is presented as it overlaps with the three molecular features used for in silico screening. Similarly, one of the mimics of IRRP-3 is also shown which interferes with the IFN-IFNAR complex formation [25]. (B) A model of the complex of IFN-IFNAR. Connolly surface spanning IRRP-3 region is shown in magenta. Key residues from IRRP-1 region, Leu30, Arg33, and Asp35 on IFN- $\alpha$ 2a and the potential interacting residues on the IFNAR2 subdomain are shown by capped stick model. IFN- $\alpha$ 2a is illustrated in a cartoon model in red and IFNAR domains are shown in blue ribbon.

torsional rotation on the molecules. A set of 1079 hits matching all three features were selected for further refinement in silico by using additional criteria, such as the number of hetero atoms in each molecule (>4 atoms), molecular weight (<700 daltons), and the number of rotatable bonds (<10). The refined set of compounds utilizing these parameters contained 153 unique molecules. Each of these molecules was visually investigated, by overlapping molecular features of each compound with the surface features of the IRRP-1 region of IFN- $\alpha$ 2a for an optimal core structure. Additionally, synthetic feasibility and nonreactive structural features were considered when determining the overall viability of the small molecule for final selection. This selection process led to a group of 11 compounds (**1–11**, Chart 1).

### 2.2. Chemistry Compounds

**1**, **2**, **4–11** were acquired from commercial sources and compound **3** was synthesized. All anhydrous reactions were performed under a nitrogen atmosphere. All solvents and reagents were obtained from commercial sources; anhydrous solvents were prepared following standard procedures. Reaction progress was monitored on TLC plates (Silica gel-60 F<sub>254</sub>). Chromatographic purifications were performed using silica gel (60 Å, 70–230 mesh). Compounds were confirmed by LC/MS and <sup>1</sup>H NMR spectroscopy. NMR spectra were recorded on a Varian spectrometer (300 and 400 MHz for <sup>1</sup>H, 75 and 100 for <sup>13</sup>C). Chemical shifts were reported in  $\delta$  ppm using tetramethylsilane (TMS) as a reference for the <sup>1</sup>H NMR spectra.

#### 2.2.1. Ethyl 4-(4,6-dioxo-5-(*o*-toluyl)-4,5,6,6a-tetrahydro-3aH-pyrrolo[3,4-*d*]isoxazole-3-carbonyl)-5-methyl-1-(*p*-toluyl)-1H-pyrazole-3-carboxylate (**1**)

<sup>1</sup>H NMR (CDCl<sub>3</sub>)  $\delta$  7.89 (d, *J* = 8.0 Hz, 2H), 7.24–7.20 (m, 4H), 7.14–7.12 (m, 3H), 6.08 (d, *J* = 5.6 Hz, 2H), 5.02 (d, *J* = 5.6 Hz, 1H),

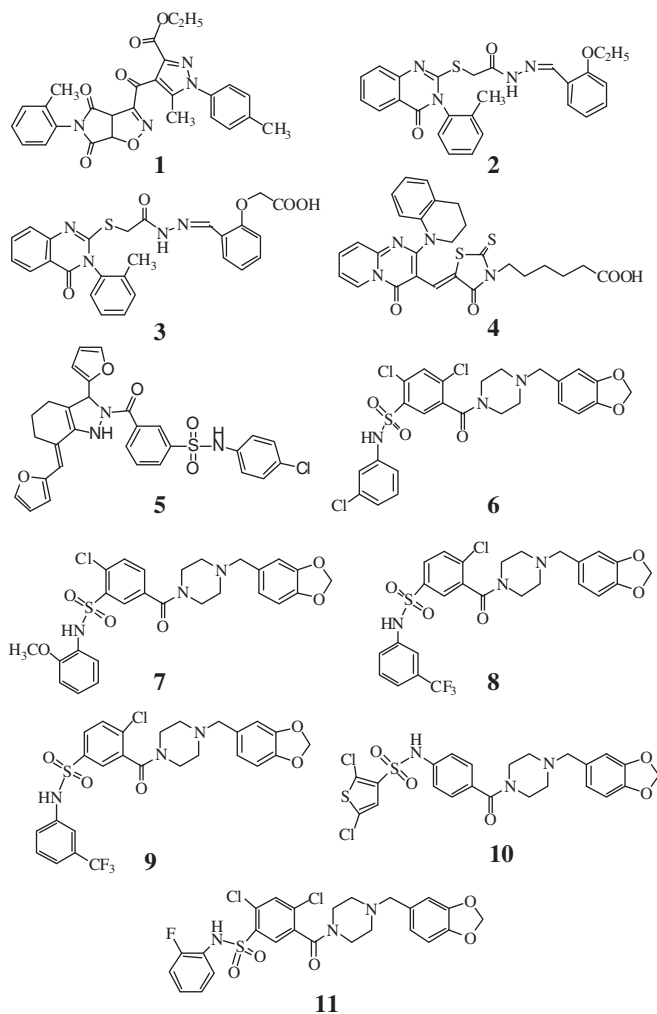


**Chart 1.** Structures of the small molecule mimics of IRRP-3 region on the surface of IFN- $\alpha$ 2a.

4.31 (q,  $J = 7.2$  Hz, 2H), 2.43 (s, 3H), 2.43 (s, 3H), 2.39 (s, 3H), 1.30 (t,  $J = 7.2$  Hz, 3H). Mass ESI ( $C_{27}H_{24}N_4O_6$ ) [ $MH^+$ ] calcd 501.1774, found. 501.2875.

### 2.2.2. *N*-(2-Ethoxybenzylidene)-2-((4-oxo-3-*o*-toluyl-3,4-dihydroquinazolin-2-yl)thio)aceto hydrazide (2)

This compound is a mixture of *E* and *Z* isomers.  $^1H$  NMR ( $CDCl_3$ )  $\delta$  8.45 (s, 1H), 8.76 (s, 1H), 8.29 (dd,  $J = 8$  and 2 Hz, 1H), 8.22 (dd,  $J = 8$  and 2 Hz, 1H), 7.88 (dd,  $J = 8$  and 2 Hz, 1H), 7.84 (dd,  $J = 8$  and 2 Hz, 1H), 7.76 (dd,  $J = 8$ , 2 Hz, 1H), 7.72 (dd,  $J = 8$ , 2 Hz, 1H), 7.59–7.33 (m, 12H), 7.26 (t,  $J = 6.4$  Hz, 2H), 6.98–6.86 (m, 4H), 4.12 (q,  $J = 7.2$  Hz, 2H), 4.05 (q,  $J = 7.2$  Hz, 2H), 3.37 (dd,  $J = 2$ , 1.6 Hz, 4H), 2.18 (s, 6H), 1.46 (t,  $J = 7.2$  Hz, 3H), 1.37 (t,  $J = 7.2$  Hz). Mass ESI ( $C_{26}H_{24}N_4O_3S$ ) [ $MH^+$ ] calcd 473.1647, found. 473.1793.

### 2.2.3. 6-(5-((2-(3,4-Dihydroquinolin-1-(2H)-yl)-4-oxo-4H-pyrido[1,2-*a*]pyrimidin-3-yl)methylene)-4-oxo-2-thioxothiazolidin-3-yl)hexanoic acid (4)

This compound is a mixture of *E* and *Z* isomers.  $^1H$  NMR ( $CDCl_3$ )  $\delta$  8.89 (ddd,  $J = 7.2$ , 1.6, 0.8 Hz, 1H), 8.21 (ddd,  $J = 7.2$ , 1.6, 0.8 Hz, 1H), 7.82 (s, 1H), 7.73–7.68 (m, 1H), 7.67 (s, 1H), 7.60 (m, 1H), 7.42–7.31 (m, 1H), 7.70–7.34 (m, 1H), 7.21–7.08 (m, 8H), 7.00 (dt,  $J = 7.2$ , 1.2 Hz, 1H), 6.88 (dt,  $J = 7.2$ , 1.2 Hz, 1H), 4.13 (t,  $J = 8$  Hz, 1H), 3.930–3.80 (m, 5H), 3.13 (t,  $J = 6$  Hz, 2H), 2.96 (t,

$J = 6$  Hz, 2H), 2.38 (d,  $J = 7.6$  Hz, 2H), 2.27 (t,  $J = 7.6$  Hz, 2H), 1.68–1.78 (m, 4H), 1.60–1.42 (m, 4H), 1.33–1.25 (m, 4H). Mass ESI ( $C_{27}H_{26}N_4O_4S_2$ ) [ $MH^+$ ] calcd 535.1474, found. 535.3018.

### 2.2.4. *N*-(4-Chlorophenyl)-3-(3-(furan-2-yl)-7-(furan-2-ylmethylene)-2,3,4,5,6,7-hexahydro-1*H*-indazole-2-carbonyl)benzenesulfonamide (5)

This compound is a mixture of *E* and *Z* isomers.  $^1H$  NMR ( $CDCl_3$ )  $\delta$  8.39 (s, 1H), 8.09 (d,  $J = 7.6$  Hz, 1H), 7.81 (d,  $J = 6.4$  Hz, 1H), 7.59–7.41 (m, 3H), 7.15–6.99 (m, 5H), 6.52–6.37 (m, 4H), 5.23 (d,  $J = 9$  Hz, 1H), 3.48–3.39 (m, 1H), 2.48–2.36 (m, 1H), 2.32–2.23 (m, 1H), 2.09–2.01 (m, 1H), 1.73–1.63 (m, 2H). Mass ESI ( $C_{29}H_{24}ClN_3O_5S$ ) [ $MH^+$ ] calcd 562.1203, found. 562.2392.

### 2.2.5. 5-(4-(Benzo[*d*][1,3]dioxol-5-yl-methyl)piperazine-1-carbonyl)-2,4-dichloro-*N*-(3-chlorophenyl)benzenesulfonamide (6)

$^1H$  NMR ( $CDCl_3$ )  $\delta$  8.07 (br s, 1H), 7.66 (d,  $J = 1.2$  Hz, 1H), 7.51 (d,  $J = 1.2$  Hz, 1H), 7.22–7.01 (m, 5H), 6.89–6.86 (m, 1H), 6.03 (s, 2H), 4.18 (br s, 4H), 3.39 (s, 2H), 1.38–1.25 (m, 4H). Mass ESI ( $C_{22}H_{22}Cl_3N_3O_5S$ ) [ $MH^+$ ] calcd 582.0424, found 582.1658.

### 2.2.6. 5-(4-(Benzo[*d*][1,3]dioxol-5-yl methyl)piperazine-1-carbonyl)-2-chloro-*N*-(2-methoxyphenyl) benzene sulfonamide (7)

$^1H$  NMR ( $CDCl_3$ )  $\delta$  7.95 (t,  $J = 1.2$  Hz, 1H), 7.56 (br s, 1H), 7.53 (d, 1.2 Hz, 1H), 7.45 (dd,  $J = 8$ , 1.6 Hz, 1H), 6.98 (dt,  $J = 8$ , 1.6 Hz, 1H), 6.85 (d,  $J = 1.2$  Hz, 1H), 6.80 (dt,  $J = 7.6$ , 1.2 Hz, 1H), 6.78–6.71 (m, 3H), 5.96 (s, 2H), 3.72 (br s, 2H), 3.72 (s, 3H), 3.44 (s, 2H), 3.17 (br s, 2H), 2.49 (br s, 2H), 2.29 (br s, 2H). Mass ESI ( $C_{26}H_{26}ClN_3O_6S$ ) [ $MH^+$ ] calcd 544.1309, found 544.1410.

### 2.2.7. 3-(4-(Benzo[*d*][1,3]dioxol-5-ylmethyl) piperazine-1-carbonyl)-4-chloro-*N*-(3-(trifluoromethyl) phenyl) benzenesulfonamide (8)

$^1H$  NMR ( $CDCl_3$ )  $\delta$  7.80 (d,  $J = 2$  Hz, 1H), 7.58 (dd,  $J = 8.4$ , 2 Hz, 1H), 7.44 (d,  $J = 8.8$  Hz, 1H), 7.39 (br s, 1H), 7.37–7.27 (m, 3H), 6.84 (br s, 1H), 6.76–6.71 (m, 2H), 5.95 (s, 2H), 3.81 (br s, 2H), 3.44 (s, 2H), 3.17–3.16 (m, 1H), 3.15–3.10 (m, 1H), 2.60–2.45 (m, 2H), 2.45–2.36 (m, 1H), 2.35–2.25 (m, 1H). Mass ESI ( $C_{26}H_{23}ClF_3N_3O_5S$ ) [ $MH^+$ ] calcd 582.1077, found 582.2308.

### 2.2.8. 3-((4-(4-Fluorophenyl)piperazin-1-yl)methyl)-*N*-(2-methoxyphenyl)-2-thioxo-2,3-dihydrobenzo[*d*]oxazole-5-sulfonamide (9)

$^1H$  NMR ( $CDCl_3$ )  $\delta$  7.73 (d,  $J = 7.2$  Hz, 1H), 7.63 (s, 1H), 7.56 (d,  $J = 7.2$  Hz, 1H), 7.35 (d,  $J = 8.8$  Hz, 1H), 7.02–6.96 (m, 3H), 6.90–6.83 (m, 3H), 6.71 (d,  $J = 8.4$  Hz, 1H), 4.99 (s, 2H), 3.61 (s, 3H), 3.05 (dd,  $J = 5.2$  and 4.8 Hz, 4H), 2.82 (dd,  $J = 5.2$  and 4.8 Hz, 4H). Mass ESI ( $C_{25}H_{25}FN_4O_4S_2$ ) [ $MH^+$ ] calcd 529.1380, found 529.1453.

### 2.2.9. *N*-(4-(4-(Benzo[*d*][1,3]dioxol-5-yl-methyl)piperazine-1-carbonyl)phenyl)-2,5-dichlorothiophene-3-sulfonamide (10)

$^1H$  NMR ( $CDCl_3$ )  $\delta$  7.35 (d,  $J = 8.8$  Hz, 2H), 7.15 (d,  $J = 8.8$  Hz, 2H), 7.07 (s, 1H), 6.84 (d,  $J = 1.2$  Hz, 1H), 6.75 (d,  $J = 7.6$  Hz, 1H), 6.720 (dd,  $J = 7.6$ , 1.2 Hz), 5.95 (s, 2H), 3.83–3.64 (br s, 2H), 3.49–3.33 (br s, 4H), 2.56–2.37 (br s, 2H), 2.361–2.274 (br s, 2H). Mass ESI ( $C_{23}H_{21}Cl_2N_3O_5S_2$ ) [ $MH^+$ ] calc. 554.0378, found 554.0330.

### 2.2.10. 5-(4-(Benzo[*d*][1,3]dioxol-5-ylmethyl)piperazine-1-carbonyl)-2,4-dichloro-*N*-(2-fluorophenyl) benzene sulfonamide (11)

$^1H$  NMR ( $CDCl_3$ )  $\delta$  7.87 (s, 1H), 7.64 (s, 1H), 7.44 (dt,  $J = 2$  and 8 Hz, 1H), 7.12–6.97 (m, 3H), 6.85 (s, 1H), 6.79–6.74 (m, 2H), 5.97 (s, 2H), 4.13–3.99 (m, 2H), 3.83–3.74 (m, 2H), 2.60–2.49 (m,

2H), 2.33–2.26 (m, 2H). Mass ESI (C<sub>25</sub>H<sub>22</sub>Cl<sub>2</sub>FN<sub>3</sub>O<sub>5</sub>S) [MH<sup>+</sup>] calcd 566.0720, found 566.0671.

### 2.2.11. *p*-Toluyyl isothiocyanate (13)

Carbon disulfide (7.8 g, 102.8 mmol) and triethylamine (1.6 g, 15.4 mmol) were dissolved in ethanol (15 mL). Then *p*-toluidine **12** (1.1 g, 10.3 mmol) in ethanol (2 mL) was added dropwise at room temperature with continuous stirring. After 6 h stirring, the reaction mixture was cooled to 0 °C, and ethyl chloroformate (1.0 g, 9.3 mmol) was added dropwise. The reaction mixture was stirred for an additional 30 min at 0 °C, and slowly warmed to 25 °C until the bubbles subsided. The reaction mixture was concentrated, dissolved in water (15 mL) and was extracted with diethyl ether (3 × 15 mL). The organic phase was dried (anhydrous MgSO<sub>4</sub>) and was concentrated to obtain the crude product **13** as a pale yellow oil (was used without further purification).

### 2.2.12. 3-(*p*-Toluyyl)-2-thioxo-2,3-dihydroquinazolin-4(1H)-one (14)

Compound **13** (2.1 g, 13.8 mmol) and 2-aminobenzoic acid methyl ester were dissolved in 50% DMSO (8 mL) and placed in a 20 mL microwave vessel. The microwave vessel was sealed and was subjected to microwave irradiation at 120 °C for 25 min. After cooling to room temperature, the crude reaction mixture was poured onto ice-water (100 mL) with vigorous stirring. The resulting solids were filtered, washed with cold water (3 × 15 mL), hexanes (3 × 15 mL) and dried under vacuum to obtain the product **14** as white powder (81% yield). <sup>1</sup>H NMR (DMSO-*d*<sub>6</sub>) δ 13.00 (s, 1H), 7.93 (d, *J* = 8.5 Hz, 1H), 7.76 (t, *J* = 7.5 Hz, 1H), 7.42 (d, *J* = 8.5 Hz, 1H), 7.32 (t, *J* = 7.5 Hz, 1H), 7.25 (d, *J* = 8 Hz, 2H), 7.12 (d, *J* = 8 Hz, 2H), 2.52 (s, 1H), 2.35 (s, 3H).

### 2.2.13. Ethyl-2-(3-(*p*-toluyyl)-4-oxo-3,4-dihydroquinazolin-2-yl)sulfanyl acetate (15)

To a solution of compound **14** (1.1 g, 3.9 mmol) in DMF (20 mL), ethyl bromoacetate (0.52 mL, 4.7 mmol) and potassium carbonate (1.9 g, 14.1 mmol) were added. The reaction was continued at 100 °C for 3 h and the mixture was triturated with cold water to yield a precipitate. The precipitate purified by flash column chromatography (gradient 0–50%, EtOAc in Hexanes) to yield compound **15** as a white powder (94% yield). <sup>1</sup>H NMR (CDCl<sub>3</sub>) δ 8.23 (d, *J* = 7.5 Hz, 1H), 7.72 (t, *J* = 7.5 Hz, 1H), 7.55 (d, *J* = 7.5 Hz, 1H), 7.40 (t, *J* = 7.5 Hz, 1H), 7.36 (d, *J* = 8 Hz, 2H), 7.24 (d, *J* = 8 Hz, 2H), 4.23 (q, *J* = 7 Hz, 2H), 3.89 (s, 2H), 2.46 (s, 3H), 1.30 (t, *J* = 7 Hz, 3H).

### 2.2.14. 2-(3-(*p*-Toluyyl)-4-oxo-3,4-dihydroquinazolin-2-yl)sulfanyl acetohydrazide (16)

Compound **15** (1.2 g, 4.3 mmol) was dissolved in ethanol (15 mL) and hydrazine hydrate (4.3 g, 86.5 mmol) was added. The reaction mixture was cooled to 0 °C, and the stirring was continued overnight at 0 °C. The precipitate from the reaction was collected by filtration and was washed with aqueous ethanol to yield compound **16** as a white solid (yield 82%). The product was used immediately for the next step without further characterization.

### 2.2.15. Ethyl 2-(2-((3-*p*-toluyyl-4-oxo-3,4-dihydroquinazolin-2-yl)sulfanyl)-acetyl hydrazinylidene) methylphenoxy)acetate (17)

Salicylaldehyde (7.21 g, 58.25 mmol) was dissolved in anhydrous acetone (50 mL) and bromoethyl acetate (10 g, 59 mmol) dissolved in acetone (10 mL) was added dropwise followed by potassium carbonate (12.30 g, 88.43 mmol). The reaction mixture was stirred at room temperature for 5 h. The crude was concentrated under vacuum, dissolved in water (50 mL) and was extracted

with dichloromethane (50 mL). The organic phase was washed with brine (2 × 10 mL) and dried (Na<sub>2</sub>SO<sub>4</sub>). The organic phase was concentrated and the crude was purified by column chromatography (0–35% EtOAc:Hexanes) to obtain ethyl 2-(formylphenoxy)acetate (72% yield). <sup>1</sup>H NMR (CDCl<sub>3</sub>) δ 10.57 (s, 1H), 7.87 (d, *J* = 8 Hz, 1H), 7.53 (t, *J* = 8 Hz, 1H), 7.09 (t, *J* = 8 Hz, 1H), 6.87 (d, *J* = 8 Hz, 1H), 4.76 (s, 2H), 4.27 (q, *J* = 7 Hz, 2 H), 1.30 (t, *J* = 7 Hz, 3H). Mass ESI (C<sub>11</sub>H<sub>12</sub>O<sub>4</sub>) [MNa<sup>+</sup>] calcd 231.0627, found 231.0636.

Then, ethyl 2-(formylphenoxy)acetate (0.3 g, 1.4 mmol) in absolute ethanol (10 mL) was added dropwise to a solution of compound **16** (0.5 g, 1.4 mmol) in absolute ethanol (20 mL). One drop of sulfuric acid was added to the reaction mixture and the reaction was refluxed for 4 h. Upon cooling the reaction to 0 °C, a precipitate was formed. The solids were collected by filtration, washed with cold ethanol (10 mL) followed by hexanes (10 mL) and dried under vacuum to yield compound **17** as a white solid (72% yield). Product was isolated as a mixture of *E* and *Z* isomers. <sup>1</sup>H NMR (CDCl<sub>3</sub>) δ 11.04 (s), 8.99 (s), 8.49 (s), 8.31 (s), 8.29 (d, *J* = 8 Hz), 8.21 (d, *J* = 8 Hz), 8.09 (d, *J* = 8 Hz), 7.93 (d, *J* = 8 Hz), 7.85–7.77 (m), 7.65 (t, *J* = 8 Hz), 7.53–7.45 (m, 1H), 7.37–7.21 (m), 7.03–6.96 (m), 6.80 (d, *J* = 8 Hz), 6.74 (d, *J* = 8 Hz), 4.69 (s), 4.57 (s), 4.48 (s), 4.30–4.21 (m), 3.86 (s), 2.46 (s), 2.44 (s), 1.32–1.24 (m). Mass ESI (C<sub>28</sub>H<sub>27</sub>N<sub>4</sub>O<sub>5</sub>S) [MNa<sup>+</sup>] calcd 531.1696, found 531.1697.

### 2.2.16. (2-(2-((3-*p*-Toluyyl-4-oxo-3,4-dihydroquinazolin-2-yl)sulfanyl)-acetyl hydrazinylidene)methyl phenoxy) acetic acid (3)

Compound **17** (0.21 g, 0.39 mmol) was dissolved in tetrahydrofuran (8 mL) and 2 N LiOH solution (1.5 mL) was added dropwise at room temperature. The reaction mixture was stirred for 18 h, solvent was removed under vacuum and the crude product was purified by flash column chromatography using a reverse phase C18 column using water as the mobile phase. Fractions with the product were concentrated and lyophilized to yield compound **3** as a white powder (33% yield). Product was isolated as a mixture of *E* and *Z* isomers. <sup>1</sup>H NMR (CD<sub>3</sub>OD) δ 8.71 (s), 8.54 (s), 8.15 (s), 8.13 (s), 7.96 (d, *H* = 8 Hz), 7.87 (d, *J* = 8 Hz), 7.82–7.74 (m), 7.68 (d, *J* = 8 Hz), 7.57 (d, *J* = 8 Hz), 7.47–7.29 (m), 6.99–6.87 (m), 4.51 (s), 4.49 (s), 3.99 (s), 2.47 (s), 2.46 (s). Mass ESI (C<sub>26</sub>H<sub>23</sub>N<sub>4</sub>O<sub>5</sub>S) [MH<sup>+</sup>] calcd 503.1383, found 503.1368.

## 2.3. Physicochemical properties

Sirius-T3 instrument (Software Version 1.1.0.10, Sirius Analytical LTD, UK) was used to determine the pK<sub>a</sub> and Log *D* properties for compounds **1–11**. Assays were performed in triplicate at 25 °C using 5 μL of 10 mM solution of each sample per assay. The dissociation constant (pK<sub>a</sub>) was determined by the Fast UV pK<sub>a</sub> experiment in the presence of neutral buffer to stabilize the pH electrode across the pH range of 2–12 during the titration of the analyte. The distribution coefficient, Log *D* was determined using the pH-metric method in which the compound was titrated for pK<sub>a</sub> in the presence of water and octanol solvent mixture, and compared to the measured aqueous pK<sub>a</sub> value.

## 2.4. Western immunoblots

Daudi cells were either left untreated, or treated with the indicated dose of IFN alfacon-1 alone or in combination with the indicated doses of test compounds, for 15 min. Cells were lysed in a phosphorylation lysis buffer supplemented with protease and phosphatase inhibitors. Equal protein aliquots were resolved by SDS-PAGE, and transferred to membranes for immunoblotting with an antibody against tyrosine phosphorylated STAT1, as described.<sup>27</sup>

## 2.5. Electrophoretic mobility shift assays (EMSA)

Daudi cells were either left untreated, treated with 100 pg IFN alfacon-1, or IFN alfacon-1 plus the indicated doses of the different test compounds, for 15 min. Nuclear extracts were prepared and reacted with  $^{32}\text{P}$ -GAS (5' AGCTTCATTTCCCGTAAATCCCT), the protein-DNA complexes resolved by native PAGE, then analyzed by EMSA, as previously described.<sup>28</sup>

## 2.6. In vitro cell viability assay

Daudi cells ( $1 \times 10^6$ ) were either left untreated or treated with the indicated doses of the specified compounds for 24 h, then washed twice in PBS, resuspended in PBS with 2% FCS and  $10^5$  cells stained with 2  $\mu\text{L}$  of propidium iodide (BD Pharmingen, 50  $\mu\text{g}/\text{mL}$ ) for 15 min. Propidium iodide stained dead cells were analyzed by FACS.

## 3. Results and discussion

In the past two decades, extraordinary steps have been taken to advance the generation of small molecule inhibitors that target PPI. A variety of tools and strategies have been applied to address the challenges of mimicking PPI.<sup>29–31</sup> However, the identification of agonists in the context of PPI, has been infrequent. Our objective is to mimic PPI between IFN- $\alpha$  and its cognate receptor by rational means, IFNAR to promote receptor activation.

Our previous studies identified three IFNAR receptor recognition sites (IRRP-1, IRRP-2 and IRRP-3) on the surface of IFN- $\alpha 2\text{a}$ , that directly interact with the two receptor subunits, IFNAR1 and IFNAR2.<sup>20,22</sup> IRRP-1 and IRRP-3 together constitute a single, contiguous surface epitope, located on one face of IFN- $\alpha 2\text{a}$ , potentially interacting with IFNAR2.<sup>32</sup> IRRP-2, on the other hand, has a much larger surface in comparison to the other IRRPs and is located on the opposite face of IFN- $\alpha 2\text{a}$ , binding to IFNAR1 (Fig. 1). The surfaces of the IRRPs cover about 27% of the total water accessible surface of IFN- $\alpha 2$ . IRRP-1 and IRRP-3 are adjacent on the surface of IFN- $\alpha$  and occupy about 17% of total surface, whereas IRRP-2, on the opposite face of IFN, occupies about 10% of the total surface. At the outset, our strategy was to mimic each of these 3 IRRPs separately as small molecules, then tether the molecules mimicking IRRP-1 or IRRP-3 with those mimicking IRRP-2, thus capturing two regions of IFN that would potentially interact with IFNAR1 and IFNAR2 (Fig. 1). To achieve this we first needed to identify the residues in the IRRPs of IFN- $\alpha 2\text{a}$  which have the greatest potential for interaction with IFNAR, and define the pharmacophore features, based on an understanding of the complex of IFN- $\alpha 2\text{a}$ -IFNAR, then use in silico screening techniques to identify ligands from chemical databases that contain these pharmacophore features.

In previous studies we used this approach to identify ligands mimicking the IRRP-3 region on the surface of IFN- $\alpha 2\text{a}$ .<sup>25</sup> Six amino acid residues on the surface of IRRP-3 were targeted for defined molecular features for in silico screening. An in-house customized small molecule library containing approximately 300,000 compounds was screened in silico for potential matches. One of the hits (NCI-619009) was chosen from this in silico screening and four analogs were synthesized. Among these compounds, two inhibited the activation of IFNAR by IFN in a dose-dependent fashion, as would be anticipated for compounds mimicking one of the IFN-IFNAR complex interactive sites (Fig. 2A).<sup>25</sup>

However, using the same approach to mimic the IRRP-1 region proved unsuccessful. Four surface residues on the IRRP-1 region, Leu30, Lys31, Arg33 and His34, were considered to define the features for in silico screening. Leu30, Lys31, Arg33 and His34 were

delineated with features of hydrophobic, cationic, cationic and hydrophobic characteristics, respectively, with the distance and volume tolerances of 1 Å. The hit molecule was refined and a small set of compounds were synthesized, but none demonstrated any potential to interfere with IFN binding to IFNAR.<sup>25</sup> In these molecules, two of the appendages on the pyrimidine core structure were carrying one hydrophobic and one cationic group, while the third appendage to the pyrimidine ring carried two key features of hydrophobic and cationic characteristics, mimicking Leu30 and Arg33, respectively. As shown in Figure 1, the interaction surfaces between IFN and IFNAR cover a large surface area, and the binding surface on IFNAR subdomains is shallow. Thus, docking protocols identify molecules to bind to IFNAR1 or IFNAR2 would not be a productive strategy. To efficiently identify small molecules mimicking the protein ligand IFN, we continue to seek to employ small molecules search protocols, and good success continues to be recorded with this tool for the identification of features in chemical structures.<sup>25,33,34</sup> The objective for this specific project is to generate molecular features mimicking the properties of surface residues and its' receptor using chemical structure databases, followed by selecting potentially useful chemical structures, complete characterizations of the chemical compounds, including re-synthesis if necessary to validate the structure, and finally confirm their biological activity unequivocally to ascertain the design principles.

Close scrutiny of our model of the IFN-IFNAR complex suggests a triad of residues in IRRP-1, Leu30, Arg33, Asp35 for further consideration for PPI mimicry.<sup>32</sup> Specifically, in light of our earlier published findings and extending our analysis, we propose that Leu30 and Arg33 should be retained as critical residues for PPI with IFNAR2, but that Lys31 and His 34 are less important, and that feature(s) of Asp35 are of greater consequence for molecular mimicry (Fig. 2B). This led to the definition of a three-distinct-features set: hydrophobic, cationic and anionic, mimicking Leu30, Arg33 and Asp35, respectively. Using this refined features set, a database of 4.1 million compounds and several steps of refinement (see Experimental Section) led to the identification of 11 compounds, 1–11 (Chart 1 and Fig. 3). These compounds generally can be classified into five distinct chemical core structures, with 1, 2–3, 4, 5 and 6–11 grouped into each of the five cores. Compound 3 was synthesized as per Scheme 1, whereas compounds 1–2 and 4–11 were acquired from commercial sources, and their structures and purity were analytically confirmed in our laboratory. Compound 3 was synthesized in seven steps from *p*-methyl aniline 13. Compound 13 was treated with ethyl bromoacetate followed by hydrazine hydrate to produce the acyl hydrazine 5 that was condensed with the benzyl aldehyde 7 to give the target compound 3. Physicochemical properties for compounds 1–11 were determined for consideration in the context of the corresponding biological activities' profiles. These compounds were evaluated for their potential to interfere with IFN activation of IFNAR, an expected outcome if these molecules are mimicking a portion of the surface features (IRRP-1) on IFN that specifically interacts with the extracellular binding site of the cell surface receptor. Specifically, for productive IFNAR activation, each of IRRP-1, IRRP-2 and IRRP-3 must contact the respective binding sites on IFNAR1 and IFNAR2 to enable receptor dimerization and subsequent intracellular activation. Any interference with IFN-IFNAR1 or IFN-IFNAR2 interactions will preclude complete receptor activation.

A series of experiments were conducted with compounds 1–11 to evaluate their potential to interfere with IFNAR activation by IFN. Binding of IFN to IFNAR activates the JAK-STAT pathway. Specifically, following IFN binding to IFNAR, the receptor-associated JAK1 and Tyk2 kinases phosphorylate tyrosine residues in the intracellular domains of IFNAR1 and IFNAR2 that serve as recruitment sites for STAT1, STAT2 and STAT3. Once recruited to the

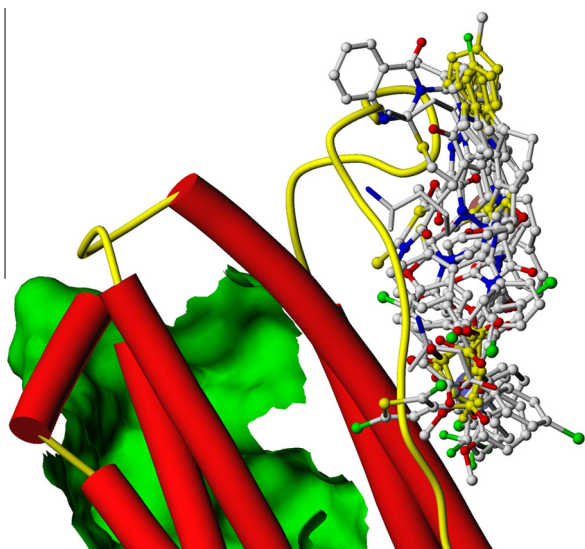


**Figure 3.** Overlap of the structures of compounds **1–11** onto the features from Leu30, Arg33 and Asp35 in IRRP-1 on the surface of IFN- $\alpha$ 2a. Compounds are shown in ball-and-stick representation, and IFN- $\alpha$ 2a in a cartoon model ( $\alpha$ -helix: red, loops and turns: yellow).

receptor, the STATs in turn are phosphorylated by the JAKs and released from the receptor. They then form homo- and hetero-dimeric STAT complexes that translocate to the nucleus to bind to interferon-stimulated response element (ISRE) and IFN- $\gamma$ -activated site (GAS, also referred to as sis-inducible elements or SIE) elements in the promoters of IFN-inducible genes, thereby activating gene transcription. We chose to evaluate two events that are a direct consequence on IFN-IFNAR interactions: (1) the IFN-inducible phosphorylation of STAT1, and (2) the formation of STAT complexes (sis-inducing factor or SIF) complexes that bind to the GAS element. Both are immediate events associated with IFNAR activation by IFN binding, and the choice of GAS element binding will specify STAT1:STAT1 complex-DNA binding, confirming any results obtained with STAT1 phosphorylation. Since, STAT1 is involved in several IFN-inducible STAT complexes (STAT1:STAT1; ISGF3; STAT1:STAT3), STAT1 was bioassayed to study the effects of the inhibitors. For these bioassays we selected IFN alfacon-1 to include in all experiments, since this novel synthetic IFN is the most potent IFN- $\alpha$  and exhibits the highest binding affinity for IFNAR.<sup>35</sup> Any inhibition of IFN alfacon-1-mediated receptor activation by a small compound would therefore indicate an optimal hit.

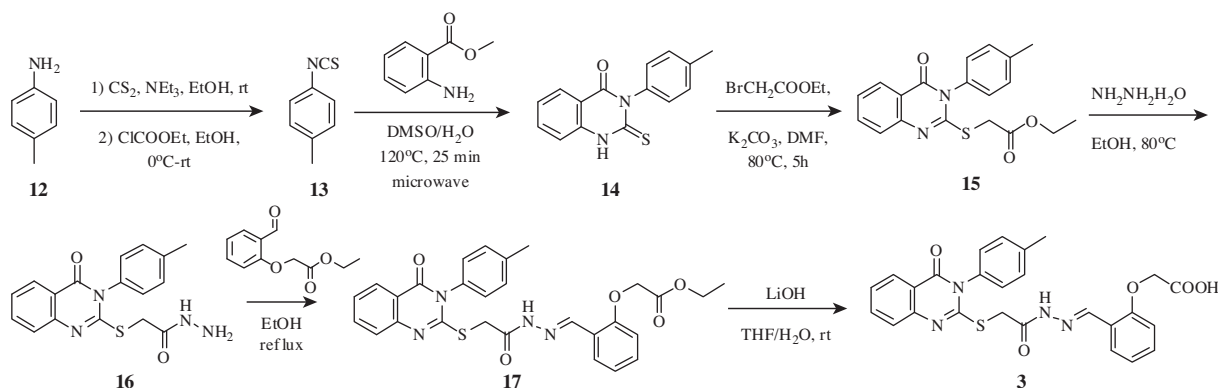
Accordingly, Daudi cells were treated with IFN alfacon-1 in the presence or absence of compounds **1–11** and whole cell lysates were analyzed for IFN-inducible phosphorylation of STAT1

(Fig. 4A and B). Compounds **3**, **4** and **10** inhibited the phosphorylation of STAT1, but other compounds did not exhibit such activity. Based on this initial screen, compounds **3**, **4** and **10** were re-examined for their ability to block IFN-inducible STAT1 phosphorylation, using nuclear extracts for analysis. The data in Figure 4, panel C, confirm the findings of our initial screen. Compound **3** was identified as the most potent inhibitor of IFN alfacon-1 activation of IFNAR, in the context of IFN-inducible STAT1 phosphorylation. Accordingly, we conducted dose-response experiments with compound **3** in the context of blocking IFN-inducible STAT1 phosphorylation (Fig. 4D).

In subsequent experiments, we evaluated compounds **3**, **4** and **10**, based on their potency, for their ability to interfere with IFN inducible STAT-DNA binding. As described above, IFN activation of IFNAR leads to STAT phosphorylation, a pre-requisite for STAT complex formation, and subsequent translocation to the nucleus and DNA binding. To confirm the effects of the IRRP-1 compound mimetics on IFN inducible STAT1 phosphorylation, we examined IFN-inducible DNA binding of STAT complexes, in an electrophoretic mobility shift assay (EMSA). Daudi cells were treated with IFN alfacon-1 in the presence or absence of compounds **3**, **4** or **10** and nuclear extracts were analyzed by EMSA for binding to an IFN- $\gamma$ -activated site (GAS/SIE) using a <sup>32</sup>P-GAS element (Fig. 5). Compounds **3**, **4** and **10** exhibited inhibition of the activation of IFNAR by IFN as seen from the reduced amounts of SIE binding. Notably, compounds **3** and **10** were more potent inhibitors of IFN-inducible STAT-DNA binding than compound **4**. These three compounds were further evaluated for cell toxicity in a 24 h assay (Supplementary Materials, Fig. S-1). Notably, compound **4** exhibited toxicity across the 0–200  $\mu$ M dose range, in contrast to compounds **3** and **10**. Our data indicate that compound **3**, mimicking the features of IRRP-1 residues, inhibits the activation of IFNAR by IFN- $\alpha$  confirming our design principles.

Compounds **6–11**, all with pKa values greater than 5.1 units (weak or strong bases) and corresponding LogD values in the range of –0.3 to 2.4, did not exhibit any activity in our assays, with the exception of **10**, but the data are confounded by the high toxicity of this compound that would affect the bioassay readouts. Compounds **3** and **4**, on the other hand, exhibited anticipated biological activities, and they bear a carboxyl moiety with pKa values in the range of 4 units. Distribution coefficient (LogD<sub>pH=7.4</sub>) for **4** is 8.9 units indicating this compound as a very nonpolar molecule. Compound **3**, on the other hand carries a carboxyl group, mimicking the Asp35 side chain, as well as a moderate solubility with LogD<sub>pH=7.4</sub> of 4.7 units (Table 1), making this the most relevant molecule mimicking the protein surface residues and the lead in biological activity evaluations.

Among the selected compounds, **3** met the criteria for all three features chosen from IRRP-1: the hydrophobic side chain of Leu30



**Scheme 1.** Synthesis of compound **3**.

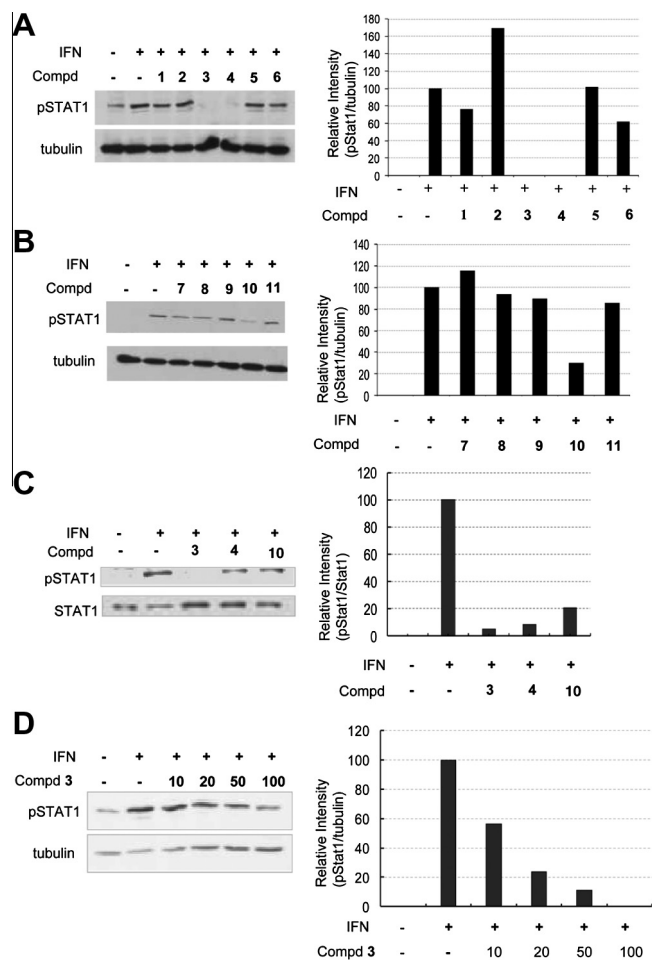


**Figure 4.** IRRP-1 mimetic compounds inhibit IFN-inducible STAT1 phosphorylation. (A) Daudi cells were either left untreated, treated with either 10 pg IFN alone, or 10 pg IFN plus 200  $\mu$ M of compounds 1–11 for 15 min. Whole cell lysates (A and B) and nuclear (C) extracts were prepared and analyzed by Western immunoblots for STAT1 tyrosine phosphorylation. The bar graphs are a quantitation of the band intensities observed, relative to the loading control, tubulin. (D) Dose–response study of whole cell extracts from Daudi cells left untreated or treated with 10 pg IFN plus compound 3 ( $\mu$ M) at the indicated doses, then analyzed by Western immunoblot for STAT1 phosphorylation.

is mimicked by the toluyl moiety at  $N^3$  of pyrimidine, the guanidinium moiety of Arg33 by the diaza moiety, and the carboxyl group of Asp35 of IFN- $\alpha$ 2 by the methyl carboxylate. Based on our studies thus far using the IRRP-1 segment of IFN, we infer that Asp35 is an important residue for the mimicry of PPI, in addition to Arg33 and Leu30, associated with productive engagement and activation of IFNAR. Interestingly, compound 2 devoid of only one carboxyl group in comparison to compound 3 did not show any inhibition of IFN binding to IFNAR. This carboxyl moiety mimics the surface residue, Asp35 in the IRRP1 portion of IFN- $\alpha$ 2a suggesting this moiety to be an important moiety for interactions with the receptor. In a recent study involving the generation of anti-IFN antibodies, it was identified that Asp35 on IFN- $\alpha$  along with another three residues including Leu30, but not Arg33, are critical for the formation of antigen–antibody complexes.<sup>36</sup> This further argues for the critical role of surface residues such as Asp35 for mimicry in protein–protein interactions while designing small molecule mimics.

With a potential mimic of IRRP-1 in the form of compound 3, and our earlier identification of an IRRP-3 mimic, we now have two small molecules mimicking the contiguous surface on IFN- $\alpha$ 2a that interacts with IFNAR2 (Fig. 2A). Studies are underway to

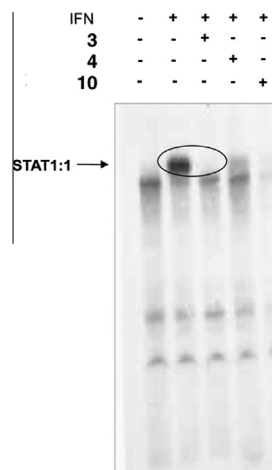


**Figure 5.** Compounds 3, 4 and 10 inhibit IFN-inducible STAT-DNA binding. Daudi cells were either left untreated or treated with 100 pg IFN in the presence or absence of test compounds (200  $\mu$ M). Nuclear extracts were prepared and analyzed by EMSA for GAS binding, using a  $^{32}$ P-labeled GAS element. Data are representative of duplicate independent experiments.

**Table 1**  
Physicochemical properties ( $pK_a$  and  $\text{Log } D_{(pH = 7.4)}$ ) for compounds 1–11

| Compound | $pK_a \pm SD$  | $\text{Log } D \pm SD$ |
|----------|----------------|------------------------|
| 1        | $9.7 \pm 0.4$  | $-0.1 \pm 0.0$         |
| 2        | $2.7 \pm 0.2$  | $5.8 \pm 0.0$          |
| 3        | $12.5 \pm 0.3$ | $4.7 \pm 0.0$          |
|          | $3.0 \pm 0.1$  |                        |
| 4        | $3.3 \pm 0.3$  | $8.9 \pm 0.0$          |
|          | $11.5 \pm 0.0$ |                        |
| 5        | $5.8 \pm 0.1$  | $-0.8 \pm 0.0$         |
| 6        | $2.9 \pm 0.1$  | $2.4 \pm 0.0$          |
|          | $9.8 \pm 0.1$  |                        |
| 7        | $9.8 \pm 0.1$  | $-0.3 \pm 0.0$         |
|          | $6.0 \pm 0.1$  |                        |
| 8        | $6.9 \pm 0.1$  | $-0.1 \pm 0.0$         |
|          | $6.0 \pm 0.3$  |                        |
| 9        | $8.1 \pm 0.0$  | $0.2 \pm 0.0$          |
|          | $6.8 \pm 0.2$  |                        |
| 10       | $6.9 \pm 0.3$  | $2.9 \pm 0.0$          |
|          | $5.1 \pm 0.0$  |                        |
| 11       | $9.1 \pm 0.0$  | $0.01 \pm 0.00$        |
|          | $6.8 \pm 0.1$  |                        |
|          | $6.1 \pm 0.1$  |                        |
|          | $6.9 \pm 0.5$  |                        |

encapsulate the hotspot regions on the entire surface of IFN- $\alpha$ 2a, i.e. mimicking IRRP-1, -2 and -3, in one non-peptidic molecule, paving the way for a potential IFN mimetic as an agonist for IFNAR.

### Acknowledgments

Authors acknowledge the financial support from the Canadian Institutes of Health Research to ENF and LPK (Grant# MOP-102527). L.P.K. acknowledges the generous support of Canada Foundation for Innovation (Leaders Opportunity Fund and Hospital Research Fund). E.N.F. is a Tier 1 Canada Research Chair. N.S. is a recipient of fellowship from Science Without Borders, Government of Brazil. Authors thank Dr. Liyakat Fatima for her excellent help with the synthesis and characterizations.

### Supplementary data

Supplementary data (cell viability data for compounds 3, 4, 10, and purity data for compounds 1–11) associated with this article

can be found, in the online version, at <http://dx.doi.org/10.1016/j.bmc.2013.12.049>.

## References and notes

- Stelzl, U.; Worm, U.; Lalowski, M.; Haenig, C.; Brembeck, F. H.; Goehler, H.; Stroedicke, M.; Zenkner, M.; Schoenherr, A.; Koeppen, S., et al. *Cell* **2005**, *122*, 957–968.
- Tucker, C. L. *Prog. Brain Res.* **2012**, *196*, 95–117.
- Jones, S.; Thornton, J. M. *Proc. Natl. Acad. Sci. U.S.A.* **1996**, *93*, 13–20.
- Oti, M.; Snel, B.; Huynen, M. A.; Brunner, H. G. *J. Med. Genet.* **2006**, *43*, 691–698.
- Al-Khoury, R.; Coulombe, B. *Expert Opin. Ther. Targets* **2009**, *13*, 13–17.
- Ryan, D. P.; Matthews, M. M. *Opin. Struct. Biol.* **2005**, *15*, 441–446.
- Kuzmanov, U.; Emili, A. *Genome Med.* **2013**, *5*, 37. <http://dx.doi.org/10.1186/gm441>.
- Ivanov, A. S.; Gnedenko, O. V.; Molnar, A. A.; Mezentssev, Y. V.; Lisitsa, A. V.; Archakov, A. I. *J. Bioinform. Comput. Biol.* **2007**, *5*, 579–592.
- Bienstock, R. J. *Curr. Pharm. Des.* **2012**, *18*, 1240–1254.
- Tan, C.; Wei, L.; Ottensmeyer, F. P.; Goldfine, I.; Maddux, B. A.; Yip, C. C.; Batey, R. A.; Kotra, L. P. *Bioorg. Med. Chem. Lett.* **2004**, *14*, 1407–1410.
- Shanmugam, M. K.; Nguyen, A. H.; Kumar, A. P.; Tan, B. K.; Sethi, G. *Cancer Lett.* **2012**, *320*, 158–170.
- Blain, J. C.; Mok, Y. F.; Kubanek, J.; Allingham, J. S. *Chem. Biol.* **2010**, *17*, 802–807.
- Samuel, C. E. *J. Biol. Chem.* **2007**, *282*, 20045–20046.
- Rizza, P.; Moretti, F.; Belardelli, F. *Autoimmunity* **2010**, *43*, 204–209.
- Maher, S. G.; Romero-Weaver, A. L.; Scarzello, A. J.; Gamero, A. M. *Curr. Med. Chem.* **2007**, *14*, 1279–1289.
- Piebler, J.; Schreiber, G. *J. Mol. Biol.* **1999**, *289*, 57–67.
- Laila, C.; Roisman, L. C.; Piebler, J.; Trosset, J. Y.; Scheraga, H. A.; Schreiber, G. *Proc. Natl. Acad. Sci. U.S.A.* **2001**, *98*, 13231–13236.
- Cutrone, E. C.; Langer, J. A. *J. Biol. Chem.* **2001**, *276*, 17140–17148.
- Kontsek, P. *Acta Virol.* **1994**, *38*, 345–360.
- Fish, E. N.; Banerjee, K.; Stebbing, N. *J. Interferon Res.* **1989**, *9*, 97–114.
- Cajejan-Feroldi, C.; Nosal, F.; Nardeux, P. C.; Gallet, X.; Guymarho, J.; Baychelier, F.; Sempe, P.; Tovey, M. G.; Escary, J. L.; Eid, P. *Biochemistry* **2004**, *43*, 12498–12512.
- Fish, E. N. *FEBS Lett.* **1995**, *365*, 87–91.
- Gombotz, W. R.; Pettit, D. K. *Bioconj. Chem.* **1995**, *6*, 332–351.
- Shaji, J.; Patole, V. *Ind. J. Pharm. Sci.* **2008**, *70*, 269–277.
- Bello, A. M.; Bende, T.; Wei, L.; Wang, X.; Majchrzak-Kita, B.; Fish, E. N.; Kotra, L. P. *J. Med. Chem.* **2008**, *51*, 2734–2743.
- SYBYL 7.3, Tripos International, 1699 South Hanley Rd., St. Louis, Missouri-63144, USA.
- Jia, D.; Rahbar, R.; Chan, R. W.; Lee, S. M.; Chan, M. C.; Wang, B. X.; Baker, D. P.; Sun, B.; Peiris, J. S.; Nicholls, J. M.; Fish, E. N. *PLoS ONE* **2010**, *5*, e13927.
- Ghislain, J. J.; Fish, E. N. *J. Biol. Chem.* **1996**, *271*, 12408–12413.
- Higueruelo, A. P.; Jubb, H.; Blundell, T. L. *Curr. Opin. Pharmacol.* **2013**, *13*, 791–796. <http://dx.doi.org/10.1016/j.coph.2013.05.009>.
- Valkov, E.; Sharpe, T.; Marsh, M.; Greive, S.; Hyvonen, M. *Top. Curr. Chem.* **2012**, *317*, 45–79.
- Labbé, C. M.; Laconde, G.; Kuenemann, M. A.; Villoutreix, B. O.; Sperandio, O. *Drug Discov. Today* **2013**, *18*, 958–968. <http://dx.doi.org/10.1016/j.drudis.2013.05.003>.
- Kumaran, J.; Wei, L.; Kotra, L. P.; Fish, E. N. *FASEB J.* **2007**, *21*, 3288–3296.
- Tervo, A. J.; Kyrylenko, S.; Niskanen, P.; Salminen, A.; Leppänen, J.; Nyrönen, T. J.; Järvinen, T.; Poso, A. *J. Med. Chem.* **2004**, *47*, 6292–6298.
- Hert, J.; Willett, P.; Wilton, D. J.; Acklin, P.; Azzaoui, K.; Jacoby, E.; Schuffenhauer, A. *J. Chem. Inf. Comput. Sci.* **2004**, *44*, 1177–1185.
- Blatt, L. M.; Davis, J. M.; Klein, S. B.; Taylor, M. W. *J. Interferon Cytokine Res.* **1996**, *16*, 489–499.
- Ouyang, S.; Gong, B.; Li, J. Z.; Zhao, L. X.; Wu, W.; Zhang, F. S.; Sun, L.; Wang, S. J.; Pann, M.; Li, C.; Liang, W.; Shaw, N.; Zheng, J.; Zhao, G. P.; Wang, Y.; Liu, Z. J.; Liang, M. *J. Mol. Med. (Berl)* **2012**, *90*, 837–846.